JOURNAL OF Applied Polymer SCIENCE

Regeneration of anion-exchange resins with Mg/Al double-metal hydroxides

Ying Wang,[1,2] Yan-Sheng Li,[1] Zhun Li[1,2]
[1]School of Environmental and Chemical Engineering, Dalian Jiaotong University, Dalian 116028, China
[2]School of Materials Science and Engineering, Dalian Jiaotong University, Dalian 116028, China
Correspondence to: Y.-S. Li (E-mail: dljtdx_huanjing@163.com)

ABSTRACT: Anion-exchange resins (AERs) were regenerated with Mg/Al double-metal hydroxides as the regenerant. Electrical conductivity breakthrough curves were adopted to estimate the relatively rapid regenerative effect of the AERs. The results show that the optimal regenerative effect of AER was obtained when the Mg/Al molar ratio was 3 and the dosages of Mg and Al hydroxides were 0.045 and 0.015 mol, respectively. The highest effluent water yield was obtained at an AER/cation-exchange resin volume ratio of 2:1. Characterization through scanning electron microscopy, X-ray diffraction, and thermogravimetry–differential thermal analysis showed that the regenerant was transformed and exhibited the distinguishing features of Mg/Al layered double hydrotalcites. Cycle experimentation showed that all calcined products effectively regenerated the fouled resins, and the regenerative mechanism was then established. © 2015 Wiley Periodicals, Inc. J. Appl. Polym. Sci. **2016**, *133*, 42928.

KEYWORDS: applications; recycling; resins; separation techniques; synthesis and processing

Received 18 June 2015; accepted 5 September 2015
DOI: 10.1002/app.42928

INTRODUCTION

Ion-exchange resins are functional polymer materials containing ion-exchange groups in crosslinked polymeric microsphere structures, and the structures include three parts: an insoluble three-dimensional reticular skeleton, functional groups linked to the skeleton, and exchangeable oppositely charged ions carried by the functional groups.[1,2] Anion-exchange resins (AERs) have been widely applied in the fields of water treatment, food, metallurgy, and nuclear industries[3–7] to remove inorganic salts[8,9] and organic compounds[10,11] in water. After ion exchange for a specific time, the reticular structure of the resin skeleton is obstructed by organic compounds[12] in most ion states and part of the colloidal state of water. Residual organic compounds cannot be completely eliminated in pretreatment processes such as clarification, coagulation, and filtration and will be adsorbed in the skeleton of AERs; thereby, the normal exchange performance of resins, which become fouled, is unavoidably affected.[13,14]

When the resins are fouled, their physical and chemical properties decrease to various extents, and a series of problems will appear constantly; these include the decline of the work-exchange capacity, the deterioration of the effluent water quality, and the increase of the operation cost. Thus, it is particularly urgent to finish the regeneration of the resins. Nowadays, acid–alkali solutions are widely adopted for the regeneration of resins. For example, traditional AER regeneration uses an alkali salt solution, such as 10% NaCl and 0.2% NaOH,[15] with a considerable amount of concentrated solution. Of course, these methods have some advantages; however, these procedures also increase the system operating and environmental costs, and this aggravates water pollution and resource waste.[16,17]

In this study, we introduced a cost-effective and environmental friendly AER method. In the entire regeneration process, acid and alkali waste liquids were not produced. The regeneration time was only 3 h, and the experimental setup was simple. The rinsing of the resins was not required, and the regenerant could also be recycled. AERs, which were used to obtain industrial demineralized water in a specific water purification system, were contaminated by organic compounds and other metal ions in this study. Mg/Al double-metal hydroxides were used to regenerate the AERs. The effects of the molar ratio and dosage of Mg/Al hydroxides and the volume ratio of the AERs and cation-exchange resins (CERs), on the resin regeneration were determined. The regenerant was characterized and analyzed through scanning electron microscopy (SEM), X-ray diffraction (XRD), and thermogravimetry (TG)–differential thermal analysis (DTA). The resin regenerative mechanism was also established.

EXPERIMENTAL

Preparation

All of the chemicals used in this study were analytical grade and were obtained from the Chinese Xilong Chemical Co., Ltd. Deionized water was used in all of the experiments. $Mg(OH)_2$ and $Al(OH)_3$ sol were prepared by the reaction of Mg/Al chloride

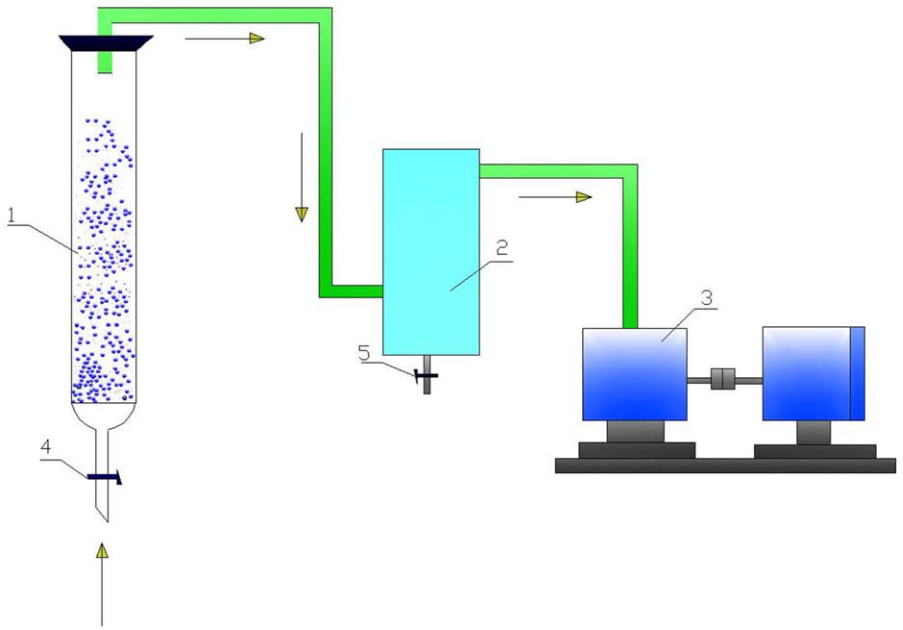

Figure 1. Schematic diagram of the experimental setup: (1) bed of resins, (2) buffer, (3) vacuum pump, and (4,5) cutoff valve. The arrows indicate the air-flow direction. [Color figure can be viewed in the online issue, which is available at wileyonlinelibrary.com.]

and NaOH, and Mg^{2+} and Al^{3+} were maintained at a certain molar ratio. The $Mg(OH)_2$ and $Al(OH)_3$ sols were rinsed until a conductivity of less than 100 μs/cm was obtained. The fouled 201 × 7 type AERs were also rinsed until a conductivity of less than 100 μs/cm was achieved. $Mg(OH)_2$, $Al(OH)_3$, and the AERs were placed into a self-made ion-exchange Plexiglas column (50 mm diameter and 400 mm height) connected to a circulating-water vacuum pump and buffer, as shown in Figure 1. Pneumatic agitation was conducted for 3 h at room temperature. Finally, the AERs and mixed suspended solids were separated. The separated resins were used for the following experiment, and the suspended solids were collected and dried for further study.

Test and Characterization

The electrical conductivity breakthrough curves were used to estimate the relatively rapid regenerative effect of the AERs. These curves were used as an indicator of the chemical equilibrium between the effluent and influent water, and this technique is a potentially simple, practical, and inexpensive method.[18]

A certain amount of 001 × 7 type CERs in the H form was regenerated through a chemical method and completely mixed with the regenerated AERs as described in the Preparation section. The mixture was then loaded into a self-made ion-exchange glass column (30 mm diameter and 300 mm height). The breakthrough reaction experiment was performed with tap water as influent water at a flow rate of 8 bed volume/h. The conductivity of water was determined in each 50 mL of effluent water with a conductivity/total dissolved solids meter (model DDS-307A, Shanghai Yoke Instrument Co., Ltd., China). As the conductivity of the influent water was 280–310 μs/cm, the breakthrough reaction experiment was terminated when the conductivity reached approximately 300 μs/cm. Moreover, the unregenerated AERs corresponded to the blank experiment.

After the reaction, the morphology of the dried regenerant was observed and analyzed through SEM (JSM-6360LV, JEOL, Japan) and thermal decomposition with a microcomputer differential thermal balance (HCT-1/2, Beijing Henven Instrument Factory, China). Effective components of the dried regenerant were then determined with an Empyrean XRD spectrometer (D8 Advance, Bruker, Germany).

RESULTS AND DISCUSSION

Determination of the Optimal Mg/Al Molar Ratio

The breakthrough curves with various Mg/Al molar ratios (2–5) are shown in Figure 2. The total molar concentration of Mg^{2+}

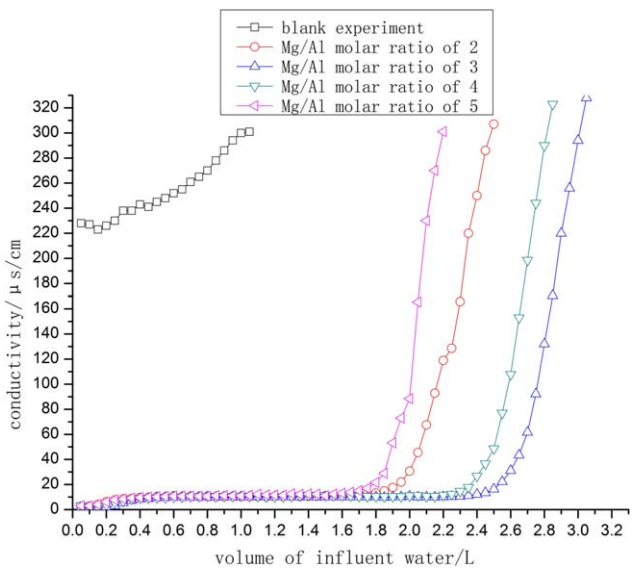

Figure 2. Breakthrough curves with various Mg/Al molar ratios. [Color figure can be viewed in the online issue, which is available at wileyonlinelibrary.com.]

and Al^{3+} was maintained at 0.06 mol. Mg/Al hydroxides could effectively regenerate the AERs, and the effluent water could be maintained for 1.7–2.4 L with a conductivity of less than 10 μs/cm when the Mg/Al molar ratio was between 2 and 5 compared with those in the blank experiment. The highest effluent water yield of 3.1 L was obtained when the Mg/Al molar ratio was 3, whereas the lowest yield was achieved when the Mg/Al molar ratio was 5. The effluent water yield was between the two extremes when the Mg/Al molar ratios were 2 and 4.

The regenerated AERs were usually contaminated with organic compounds in most ion states and part of the colloidal state in raw water. These organic compounds were mainly composed of C, H, and O and could be removed through the regeneration of the AERs and with mixed hydroxides with a solid scrub. With the aid of OH^- dissociation, the Mg/Al hydroxides in water underwent a replacement reaction with exchangeable groups in the resin or organic compounds in the resin reticular structure; this resulted in the production of Mg/Al layered double hydrotalcites, namely, Mg/AlLDHs (the characterization results confirmed that the regenerant was transformed into typical Mg/AlLDHs after the reaction, as discussed later in the Characterization and Analysis of the Regenerant section), and the recovery of the ion-exchange capacity. In addition, according to the precipitation mechanism, Mg/AlLDHs should be the compounds or symbiotic products of the two different hydroxides.[19] When the Mg/Al molar ratio was within a certain range, Mg/Al hydroxides were dehydrated and compounded easily. Part of the compounds served as a basis of nucleation. Metal ions in the solution were constantly migrated, adsorbed, and associated with the surface of the compounds with $Mg(OH)_6^{4-}$ and $Al(OH)_6^{3-}$ as growth units to increase the particle size.

In the classic Mg/AlLDH chemical structure, namely, $[Mg_6Al_2(OH)_{16}CO_3]\cdot 4H_2O$, the Mg/Al molar ratio was 3. Yang *et al.*[20] found that nucleation was easy, and the stable hydrotalcite phase was rapidly formed at an Mg/Al molar ratio of 3. Hence, the experimental results agreed with the original theory.

These analysis results suggested that the optimum Mg/Al molar ratio for the regeneration of AERs was 3.

Determination of the Optimal Volume Ratio of the AERs and CERs

The regeneration process influenced the regeneration effect of the AERs, the regeneration effect was characterized by the AER/CER electrical conductivity breakthrough experiment, and the AER/CER volume ratio was very important in the breakthrough experiment. So, we needed to determine the optimal AER/CER volume ratio and characterize the regeneration degree of the AERs. Figure 3 illustrates the breakthrough curves of the effluent water with the AERs (50, 50, and 25 mL) and CERs (50, 25, and 50 mL) at AER/CER volume ratios of 1:1, 2:1, and 1:2. The trend of the three curves was consistent for approximate volumes of the effluent water, which were maintained at a conductivity of less than 10 μs/cm for 22, 29, and 18 times the volume of the mixed resin bed, respectively. A comparison of the two curves at AER/CER volume ratios of 1:1 and 2:1 showed that the change in the resin amount did not affect the treatment effect of the tap water. A comparison of the two curves at AER/CER volume ratios of 2:1 and 1:2 showed that the increase in the AER amount intensified the treatment effect of the tap water; that is, the AERs played a decisive role. Therefore, in the water-treatment industry, a ratio of 2:1 is required as the volume ratio for AERs and CERs rather than ratios of 1:1 or 1:2. The use of Mg/Al double-metal hydroxides as a regenerant also completely restored the exchange capacity of the fouled AERs and was important in regeneration.

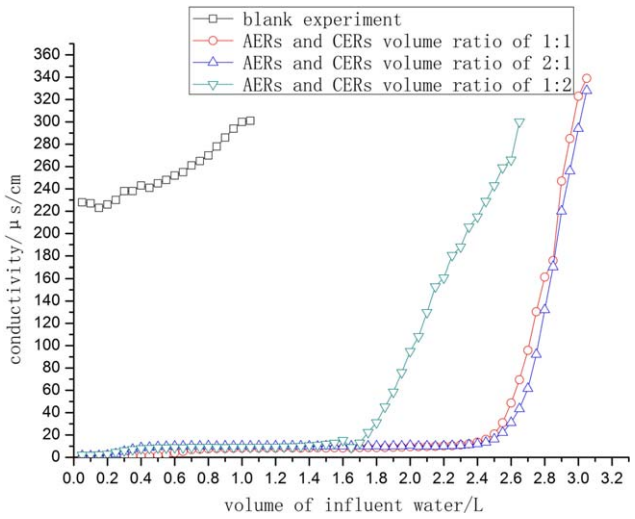

Figure 3. Breakthrough curves with different AER/CER volume ratios. [Color figure can be viewed in the online issue, which is available at wileyonlinelibrary.com.]

Thus, the optimal AER/CER volume ratio was 2:1, as determined on the basis of the results and water-treatment cost.

Determination of the Optimal Dosages of Mg/Al Hydroxides

Figure 4 shows the breakthrough curves with different dosages of Mg/Al hydroxides with an Mg/Al molar ratio of 3. The different dosages of Mg/Al hydroxides regenerated the fouled resin under pneumatic agitation, and the effluent water volume (conductivity < 300 μs/cm) reached 2.7–3.1 L. The effluent water yield was the highest at 42 times the mixed resin bed volume when $Mg(OH)_2$ and $Al(OH)_3$ were 0.045 and 0.015 mol, respectively, compared with those of the other dosages of Mg/Al hydroxides.

As low dosages of Mg and Al hydroxides, such as 0.03 and 0.01 mol, respectively, were insufficient to react with the exchangeable groups in AERs, only a part of the organic compounds was replaced into the solution or in the Mg and Al hydroxide mixed sol; this could not completely restore the exchange capacity. At high Mg and Al hydroxide dosages, namely, 0.18 and 0.06 mol, respectively, Mg/Al hydroxides adequately contacted and reacted with the resin beads. However, the used regenerant, as a kind of sol, inevitably surrounded the exchangeable ions and thereby prevented the dissociated ions from approaching the exchangeable groups, such as the organic compounds. Consequently, the exchange capacity of the resin was not fully restored, and it decreased the effluent water yield.

Therefore, the optimal doses of Mg and Al hydroxides to regenerate the fouled AERs were 0.045 and 0.015 mol, respectively.

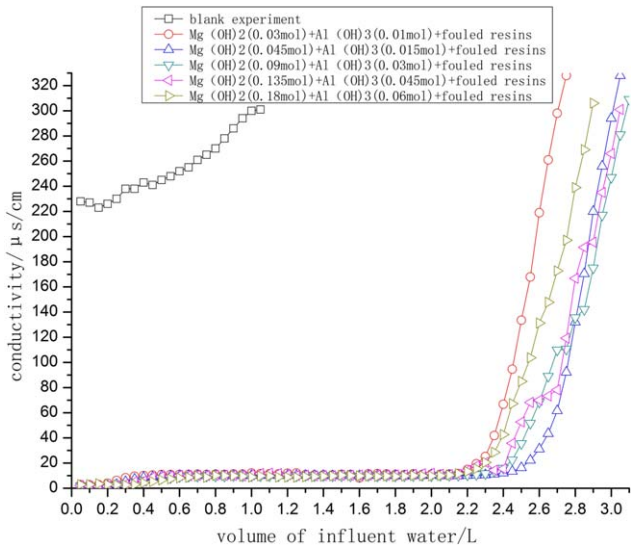

Figure 4. Breakthrough curves with different Mg/Al hydroxide dosages. [Color figure can be viewed in the online issue, which is available at wileyonlinelibrary.com.]

Characterization and Analysis of the Regenerant

After the reaction, the regenerant was characterized through SEM, XRD, and TGA–DTA. The microstructure, composition, and thermal decomposition were analyzed to confirm the performance of the regenerant.

Figure 5 shows the SEM image of the regenerant after the reaction at 5000× magnification. The regenerant showed a flat flake structure and good dispersibility with a neat morphology. The largest diameter of the flake structure was approximately 2 μm. The mean thickness of the flake structure was roughly 100 nm. The layered morphology of hydrotalcite was distinct.

The XRD patterns in Figure 6 demonstrate the typical diffraction peaks at 2θ values of 11.53, 23.21, 34.47, 38.44, 45.31, 60.68, and 62.07°. The patterns agreed with the standard card in No. 14-0525 Powder Diffraction File (PDF), namely, $[Mg_6Al_2(OH)_{16}CO_3]\cdot 4H_2O$. These results suggest that the lamellate layers were well crystallized. However, the diffraction peaks

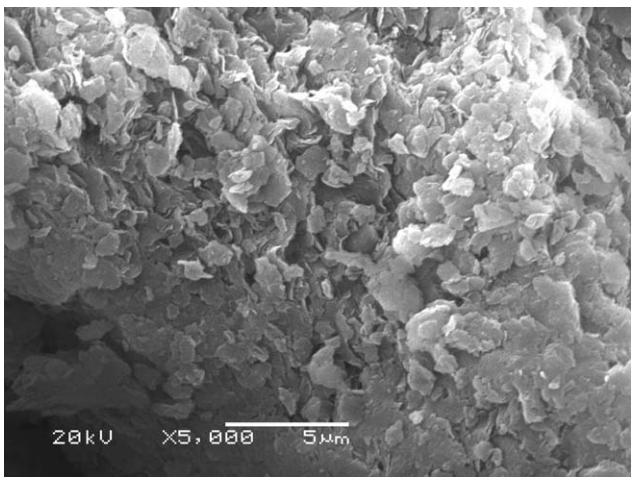

Figure 5. SEM image of the regenerant after the reaction.

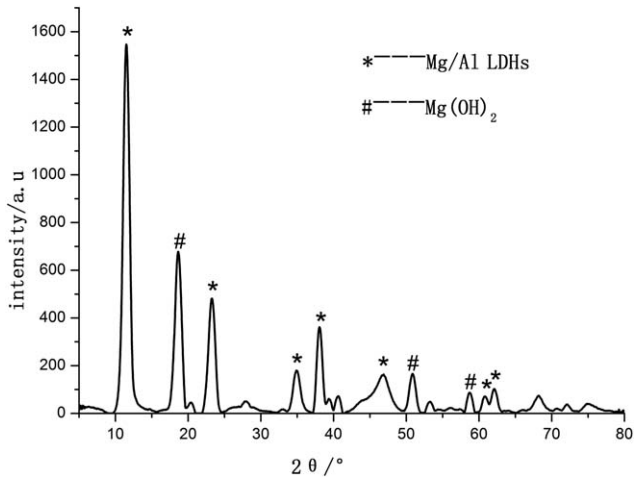

Figure 6. XRD patterns of the regenerant after the reaction.

of $Mg(OH)_2$ at 2θ values of 18.59, 50.85, and 58.64° were still observed from the patterns; this indicated that the regenerant after the reaction produced a small amount of $Mg(OH)_2$. In any case, these results could explain why the regenerant was converted into Mg/AlLDHs after it reacted with the fouled AERs.[21]

TGA–DGA was performed to analyze and identify the composition of the regenerant after the reaction (Figure 7). The thermal decomposition of the regenerant showed two obvious weight loss steps: one at 100–248.9°C, which was due to the hydrotalcite layer adsorption and crystallization water-desorption process and resulted in a 14.4% weight loss, and one at 248.9–582.1°C, which corresponded to the decomposition and desorption of a part of the CO_3^{2-} between the layer boards and OH^- on the layer boards and resulted in a 23.9% weight loss.[22] The results of thermal analysis show that the regenerant presented typical characteristics of Mg/Al hydrotalcite pyrolysis after the reaction.

The characterization and thermal analysis results of the regenerant showed that it was transformed to typical Mg/AlLDHs from Mg/Al double-metal hydroxides.

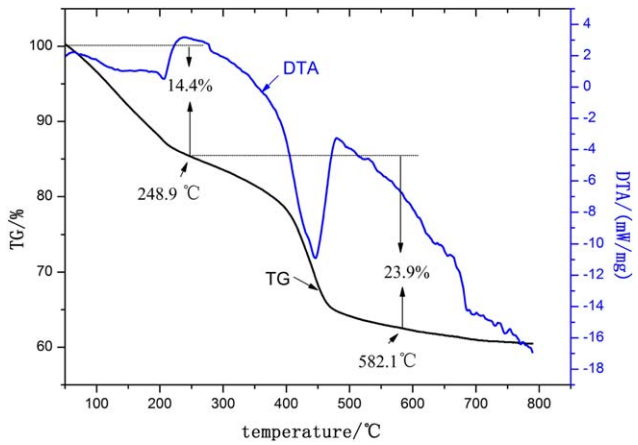

Figure 7. TG–DTA curves of the regenerant after the reaction. [Color figure can be viewed in the online issue, which is available at wileyonlinelibrary.com.]

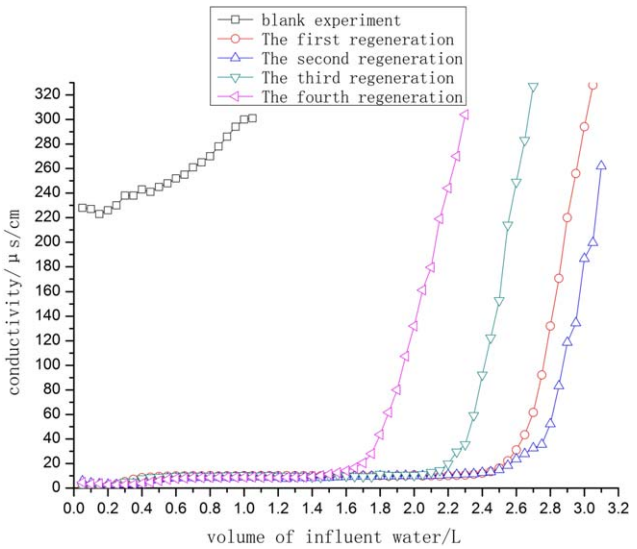

Figure 8. Breakthrough curves of cycle experimentation. [Color figure can be viewed in the online issue, which is available at wileyonlinelibrary.com.]

Cycle Experimentation

After the reaction, the regenerant was dried and calcined at 450°C for 4 h to evaluate the calcination memory of the Mg/AlLDHs.[23–25] The calcined product, namely, Mg/Al double-metal oxide, was then reacted with the AERs to achieve the recycling or sustainable consumption of the regenerant. The breakthrough curves were tested, and the cycle experiment was conducted three times. The results are shown in Figure 8.

Four cycle experiments effectively regenerated the AERs (Figure 8). The optimal result was obtained during the second regenerative effect at 3.2 L of effluent water with a conductivity of less than 300 μs/cm; this was followed by the first (3.2 L), third (2.7 L), and fourth (2.2 L) cycles. During the first regeneration cycle, part of the Mg/Al hydroxides remained uninvolved in the reaction; thus, AER could not be completely regenerated at this point. The second regeneration cycle achieved comprehensive regeneration. During this cycle, part of the regenerant was dissolved in water; this resulted in the loss of ions. A certain amount of regenerant was also adsorbed by the AERs and retained inside the resin beads. In addition, during the regeneration process without any extra regenerant added and with increased regeneration number, the amount of calcined Mg/Al double-metal oxide gradually decreased. Consequently, the regenerant that participated in the regeneration decreased. Therefore, the effluent water yield gradually decreased with increasing cycle time. Nevertheless, the addition of a certain amount of Mg/Al hydroxide to the regenerant before each cycle enhanced the regenerative effect. This phenomenon is worthy of further study and exploration.

Discussion of the Regenerative Mechanism

The regenerative mechanism was established. After the $Mg(OH)_2$ and $Al(OH)_3$ sols were completely mixed, they were reassembled in the $Mg_6Al_2(OH)_{16}\cdot(OH)_2$ form to dissociate OH^-. After the reassembled product fully contacted the resin beads under pneumatic agitation, the dissociated OH^- entered the solution, penetrated the resin beads, and underwent a replacement reaction with organic compounds in the resin beads. Finally, OH^- was displaced into the resin groups to restore the ion-exchange capacity of the AERs. The replaced organic compounds entered the solution and combined with $[Mg_6Al_2(OH)_{16}]^{2+}$ to generate $[Mg_6Al_2(OH)_{16}CO_3]\cdot 4H_2O$. This is shown in diagram form in Figure 9.

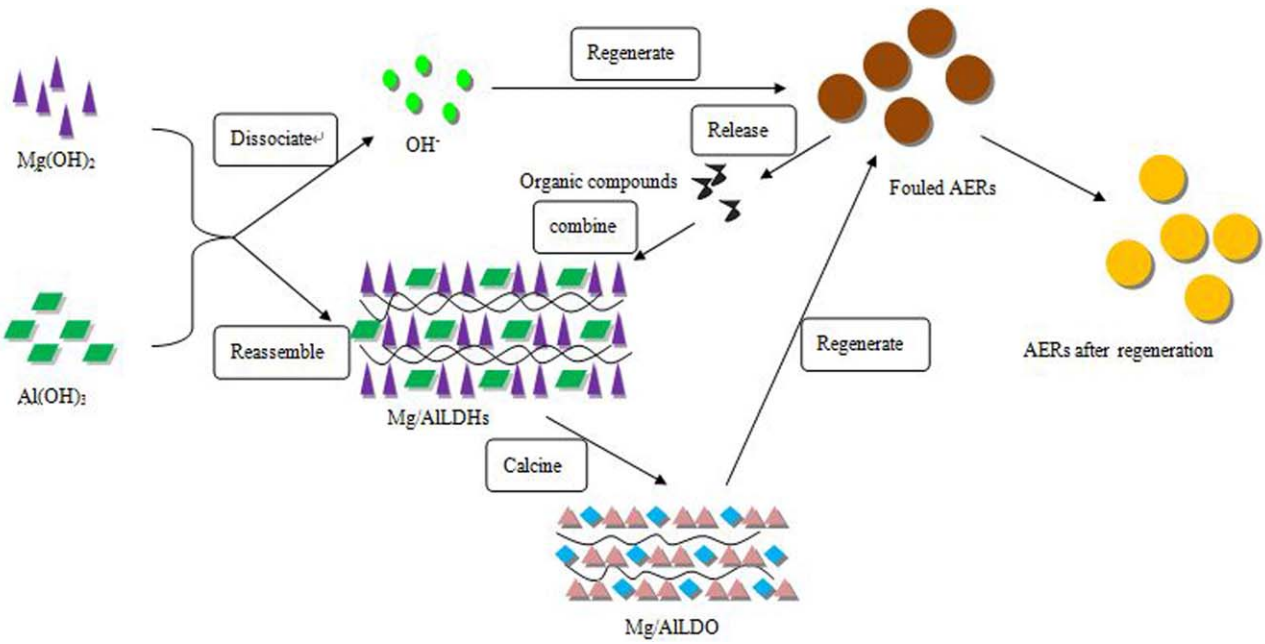

Figure 9. Schematic diagram of the resin regenerative mechanism. Mg/AlLDO = Mg/Al layered double oxides. [Color figure can be viewed in the online issue, which is available at wileyonlinelibrary.com.]

CONCLUSIONS

First, Mg/Al double-metal hydroxides regenerated fouled AERs under pneumatic agitation for 3 h. The regenerated AERs were mixed with CERs with tap water as the influent water, and the electrical conductivity breakthrough curves were tested. The results show that the optimal regenerative effect of the AERs was obtained when the Mg/Al molar ratio was 3 and the dosages of Mg and Al hydroxides were 0.045 and 0. 015 mol, respectively. The highest effluent water yield was 42 times higher than that of the mixed resin bed volume and obtained at an AER/CER volume ratio of 2:1.

Second, characterization through SEM, XRD, and TG–DTA showed that the regenerant was transformed and exhibited the distinguishing feature of the Mg/AlLDHs. The regenerant was calcined after the reaction, and the fouled resins were regenerated again to evaluate the calcination memory of the Mg/AlLDHs. Cycle experiments were then conducted. The results show that all of the calcined products effectively regenerated the fouled resins.

Third, the resin regeneration mechanism was established. The Mg/Al hydroxides mixed, reassembled, and generated OH^-. OH^- entered and replaced the organic compounds in the resin beads. $[Mg_6Al_2(OH)_{16}CO_3]\cdot 4H_2O$ was produced, and OH^- was displaced in the resin groups to restore the ion-exchange capacity of the AERs.

REFERENCES

1. Zou, J. H.; Dai, Q.; Wang, J. H.; Liu, X.; Huo, Q. *J. Nanosci. Nanotechnol.* **2007**, *7*, 2382.
2. Fulara, H.; Chaudhary, S.; Kashyap, S. C.; Pandya, D. K. *Nanosci. Nanotechnol. Lett.* **2012**, *4*, 651.
3. Rivas, B.; Quilodrán, B.; Quiroz, E. *J. Appl. Polym. Sci.* **2004**, *92*, 2908.
4. Untea, I.; Tudorache, E.; Neagu, V. *J. Appl. Polym. Sci.* **2002**, *86*, 2093.
5. Coca, M.; Mato, S.; Gonzalez-Benito, G.; Uruena, M. A.; Garcia-Cubero, M. T. *J. Food Eng.* **2010**, *97*, 569.
6. Riveros, P. A. *Hydrometallurgy* **2004**, *72*, 279.
7. Remy, E.; Picart, S.; Grandjean, S.; Delahaye, T.; Heriet, N.; Allegri, P.; Dugnr, O.; Podor, R.; Clavier, N.; Blanchart, P.; Ayral, A. *J. Eur. Ceram. Soc.* **2012**, *32*, 3199.
8. Madlen, P.; Eckhard, W.; Volker, E. *Desalination Water Treat.* **2014**, *52*, 2987.
9. Nur, T.; Johir, M. A. H.; Loganathan, P.; Vigneswaran, S.; Kandasam, J. *Desalination Water Treat.* **2012**, *47*, 50.
10. Magdalena, G.; Zbigniew, H. *Desalination* **2011**, *278*, 219.
11. Khan, M. H.; Ha, D. H.; Jung, J. Y. *Desalination Water Treat.* **2014**, *52*, 2433.
12. Pavel, K.; Katerina, K.; Miroslav, S. *Sep. Sci. Technol.* **2014**, *49*, 2352.
13. Mamchenko, A. V.; Dmitrenko, Y. A.; Kushnir, T. V. *J. Water Chem. Technol.* **2010**, *32*, 341.
14. Benedicte, P.; Imen, A.; Franck, M.; Jerzy, Z. *Environ. Sci. Pollut. Res.* **2014**, *21*, 9334.
15. Jackson, M. B.; Bolto, B. A. *React. Polym.* **1990**, *12*, 277.
16. Li, Y. S.; Wen, Y.; Cao, K.; Xu, S. F. *Dalian Railway Inst.* **1998**, *19*, 40.
17. Greenleaf, J. E.; SenGupta, A. K. *Solvent Extr. Ion Exch.* **2012**, *30*, 350.
18. Charles, D. S.; Michael, A. M.; Michael, A. M.; Roslyn, T. S. *J. Geotech. Geoenviron.* **1999**, *4*, 260.
19. Gou, G. J. M.S. Thesis, Chinese Academy of Sciences, **2005**.
20. Yang, Z. Y.; Zhang, H. W.; Zhou, J. C.; Cao, W. L. *Acta Phys. Chim. Sin.* **2007**, *23*, 795.
21. Liao, L. B.; Zhao, N.; Xia, Z. G. *Mater. Res. Bull.* **2012**, *47*, 3897.
22. Valente, J. S.; Rodriguez-Gattorno, G.; Valle-Orta, M.; Torres-Garcia, E. *Mater. Chem. Phys.* **2012**, *16*, 621.
23. Yang, Z. Q.; Mo, Z. H.; Niu, X. *Sep. Sci. Technol.* **2015**, *50*, 99.
24. Seyoon, Y.; Juhyuk, M.; Sungchul, B.; Duan, X. N.; Emmanuel, P. G.; Paulo, M. M. *Chem. Phys.* **2014**, *145*, 376.
25. Liu, J. P.; Li, Y. Y.; Huang, X. T.; Li, G. G.; Li, Z. K. *Adv. Funct. Mater.* **2008**, *18*, 1448.